BNL-222354-2021-TECH
C-A/AP/656

Summary of the CeC Experiment in RHIC Run 21

G. Wang

October 2021

Collider Accelerator Department
Brookhaven National Laboratory

U.S. Department of Energy
USDOE Office of Science (SC), Nuclear Physics (NP) (SC-26)

DISCLAIMER

Summary of the CeC Experiment in RHIC Run 21

G. Wang, V.N. Litvinenko, I. Pinayev, Y. Jing, D. Kayran, J. Ma, I. Petrushina, M. Sangroula, K. Shih, Y.H. Wu,

Abstract

The coherent electron cooling (CeC) experiment at RHIC is crucial for determining the feasibility of this technique for cooling the hadron beam in the electron-ion collider (EIC) and reaching the luminosity of 10^{34} cm $^{-1}s^{-1}$. During RHIC Run 21, various progresses have been made including successfully commissioning the time resolved diagnostic beam line (TRDBL), achieving the key performance parameters (KPP) of the system and the development of novel methods for accurate alignment of the electron beam with the ion beam. While the longitudinal cooling of the ion beam with cooling time of 100 hours was observed during Run 21, it was related to the traditional electron cooling since the cooling rate was not as sensitive to the energy of the electron beam as what one would expect from the CeC. In Run 21, we were not able to observe the longitudinal cooling of the ion beam caused by CeC and the main challenges are identified as the insufficient stability of the electrons' energy. The sources of the energy jitter have been identified and we are making improvements to the stability of the CeC system for Run 22.

Introduction

The strong hadron cooling (SHC) is needed to reach the luminosity of 10^{34} cm $^{-1}s^{-1}$ in the electron ion collider (EIC). The CeC, as a major candidate of the SHC technique to be used in EIC, has not been demonstrated experimentally and hence the ongoing proof of principle experiment of CeC at RHIC is crucial for investigating its feasibility for reaching the luminosity goal of EIC.

The CeC system has been built and commissioned during FY14 to FY17. In RHIC Run 18, we started the experiment to demonstrate the FEL-based CeC, which was not completed since the aperture of the helical wigglers was insufficient for RHIC Run 19 with 3.85 GeV/u Au ion beams. During Run 18, we discovered a new type of instability in the low energy beam transfer line (LEBT) of the CeC system, the plasma cascade instability (PCI), which led to a significant increase of the noise in the electron beam and present a major challenge for demonstrating cooling. The instability has been studied extensively and in RHIC Run 19, we were able to demonstrate the suppression of the PCI by properly adjusting the focusing elements in the LEBT. In addition, we found that the PCI mechanism can be applied to the amplification process of the CeC and based on this concept, we proposed a new CeC scheme with an amplifier based on the PCI, i.e. the Plasma-Cascade Amplifier (PCA) based CeC. Since the PCA section only requires solenoids with sufficient apertures for the low energy RHIC operation, we removed the wigglers and installed seven solenoids to test the PCA-based CeC. The PCA-based CeC system was built and commissioned in FY19-20. We started the PCA-based CeC experiment in Run 20. During Run 20,

we demonstrated the high gain plasma cascade amplification and observed the presence of ion imprinting in the electron beam.

New time-resolved diagnostic beamline (TRDBL) has been built during FY20 and successfully commissioned during Run 21. With the help of the TRDBL, we were able to achieve the key performance parameters (KPP) established for run 21. During this run, we have also developed a process for accurate alignment of the electron beam with the ion beam and a novel method of electron beam energy measurement at the cooling section with accuracy of 0.2%. The alignment of the orbit and the energy of the two beams have been confirmed with the strong signal from the recombination monitor and the longitudinal cooling of the ion bunch interacting with the electrons. However, the cooling time is in the orders of 100 hours which is at least one order of magnitude slower that what expected from the CeC. In addition, the cooling rate was not as sensitive to the energy of the electrons as one would expect from the CeC, indicating that the cooling was traditional electron cooling instead of the CeC. In the following sections, we will summarize the progresses as well as findings from the CeC experiment in RHIC run 21.

Commissioning of the TRDBL

The TRDBL locates in the straight section downstream of the first bending magnet as shown in Fig.1 for an illustration and Fig.2 for the photo of the installed system. After being accelerated to its top energy in the 704MHz accelerating cavities, the electron beam is delivered to the TRDBL if the first bending magnet is turned off.

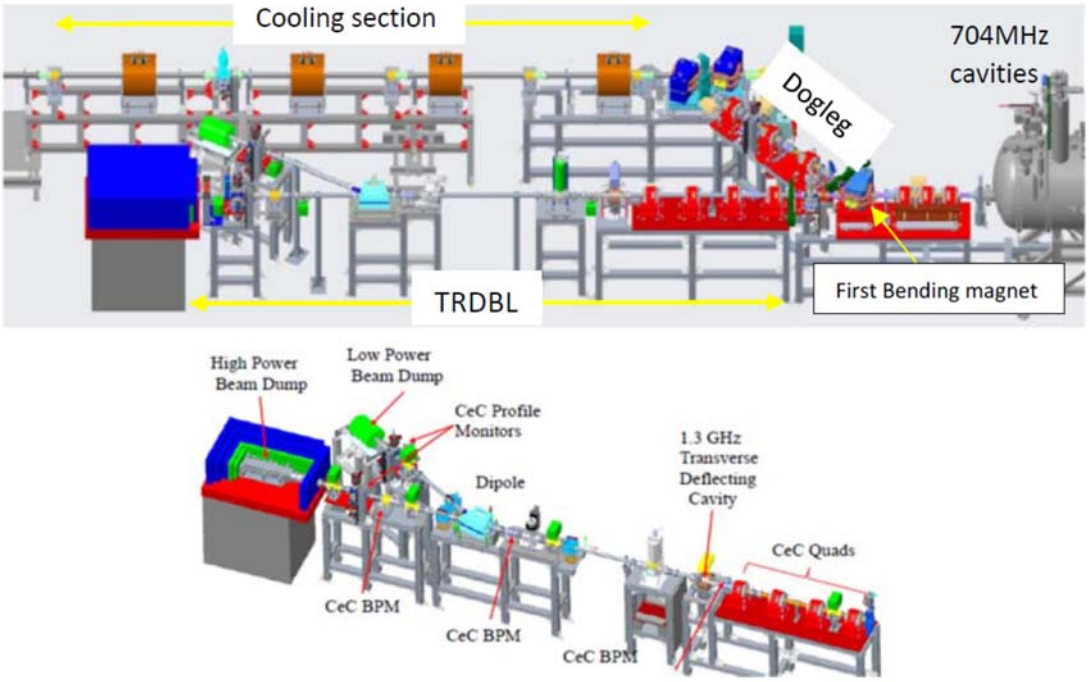

Figure 1: Overall layout (Top) and detailed illustration (Bottom) of the time-resolved diagnostic.

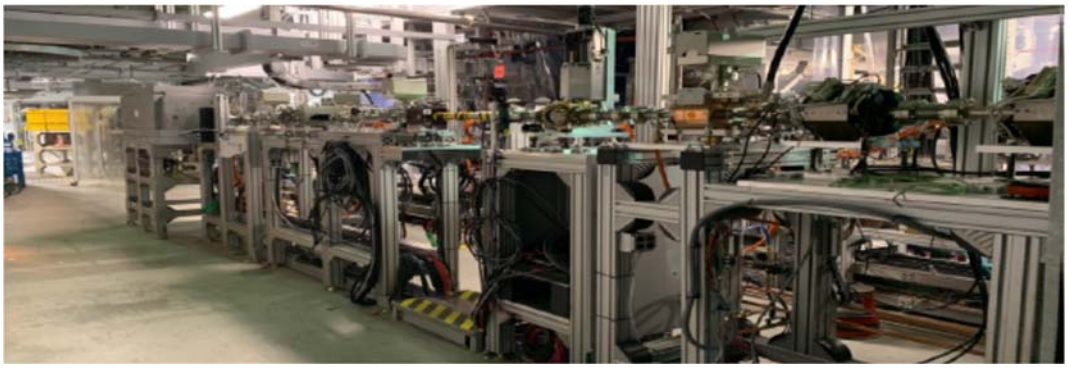

Figure 2: Photo of the installed time-resolved diagnostic beam line.

In the TRDBL, the electron beam goes through four quadrupoles (see fig. 1(bottom)) where its shape is optimized for beam diagnostics. A time dependent vertical kick is then applied to the electron beam in the 1.3 GHz deflecting cavity so that different longitudinal slices of the electron bunch move with different vertical velocities and get separated downstream in the vertical plane. For slice emittance measurement, the bending magnet downstream of the deflecting cavity is turned off and the electron beam is measured at the beam profile monitor in front of the high-power beam dump, i.e. diagnostic YAG 1. For longitudinal phase space imaging and slice energy spread measurement, the bending magnet is turned on and the electron beam reaches the beam profile monitor in front of the low power beam dump, i.e. diagnostic YAG 2.

Fig. 3 shows an example of the longitudinal beam profile measurement at the beam profile monitor in front of the high-power dump. The peak current measured for this specific example is 52 A with FWHM of 30 ps.

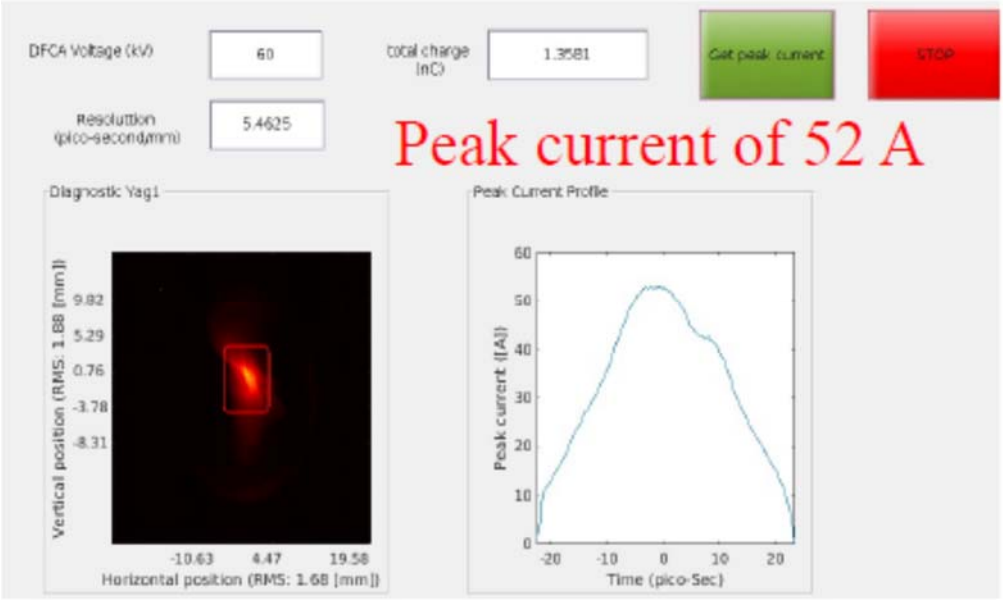

Figure 3: Screen shot of the Matlab application developed for measuring the longitudinal profile (Left) and the transverse emittance of the electron bunch (Right).

The slice emittance is measured by scanning two quadrupoles upstream of the deflecting cavity. Fig. 4 shows an example of the slice emittance measurement. For this example, the normalized projected emittance is $2\mu m$ and the slice emittance around the bunch center is about $1.5\mu m$.

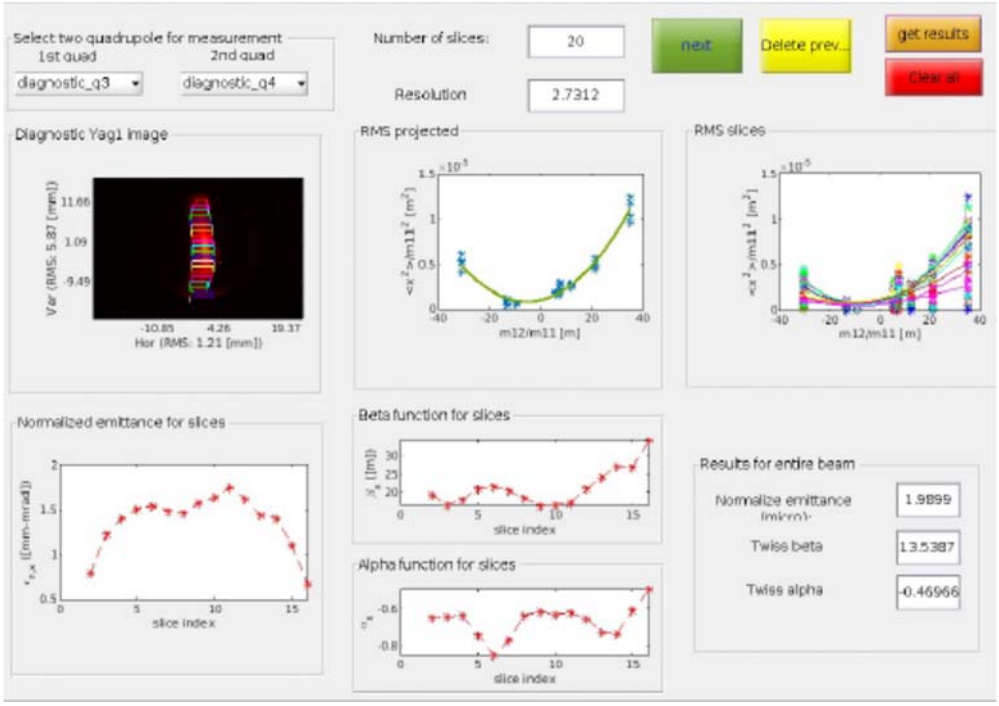

Figure 4: Screen shot of the Matlab application developed for measuring the slice emittance of the electron bunch.

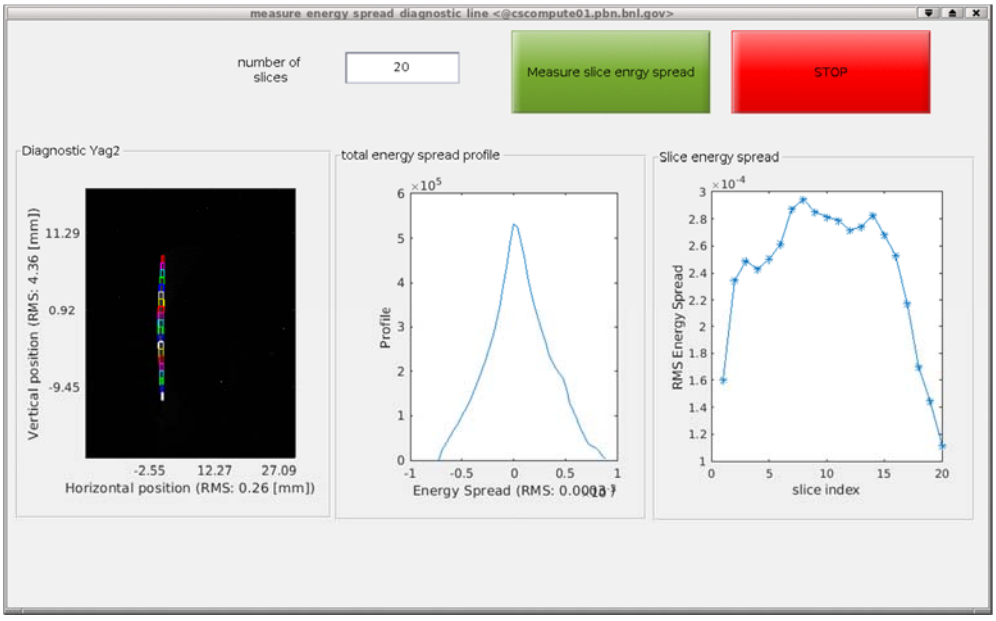

Figure 5: Screen shot of the Matlab application developed for measuring the slice energy spread of the electron bunch.

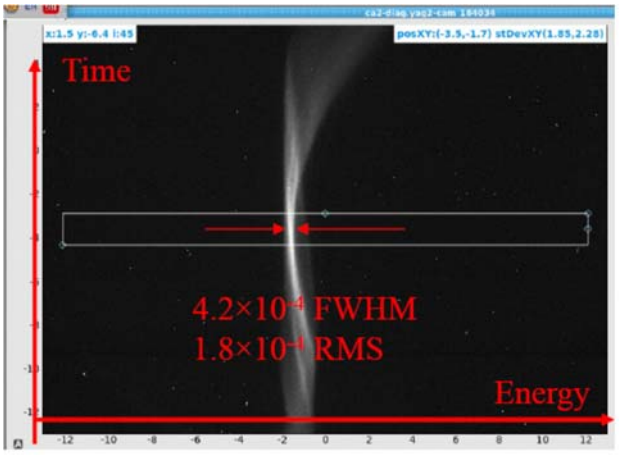

Figure 6: The longitudinal phase space image of the electron beam as measured at the YAG screen in front of the low energy dump of the TRDBL. The horizontal position corresponds to the energy of the electrons and the vertical position corresponds to the longitudinal position of the electrons in the bunch.

Fig. 5 shows an example of the slice energy spread measurement with the RMS slice energy spread of 2.8×10^{-4} around the bunch center. A screen shot of the longitudinal phase space image taken at the diagnostic YAG 2 is shown in fig. 6. For the set-up in fig. 6, the measured RMS energy spread at the bunch center was 1.8×10^{-4}.

Energy measurement of the electron beam in the cooling section

We have developed procedure for measurement of the beam energy based on rotation of the betatron motion plane by solenoid. In the original application the beam position was changed by a trim upstream of a solenoid with two current setpoints of opposite sign. Such approach allows beam to be tightly focused on a profile monitor and observe change of the beam trace with solenoid current change.

The high-current solenoids utilized in the common section do not have bipolar power supply and procedure was modified accordingly. Beam position is observed on the common section profile monitor placed after the solenoid 3. Beam scan is provided by trims 4 located between solenoids 2 and 3. The first scan is performed with solenoid 3 focusing beam on the profile monitor. The second scan is done with the third solenoid at zero and focusing is provided by solenoid 2. We have modified the trim scan as well. We are performing 4N measurements with the first N and the last N points at one trim setting and the middle 2N measurements with different trim setting. Such scan improves precision of rotation angle measurement since the beam position is observed at maximal deflection and linear drifts are suppressed.

Fig. 7 shows one example of the energy measurement of the electron beam in the cooling section.

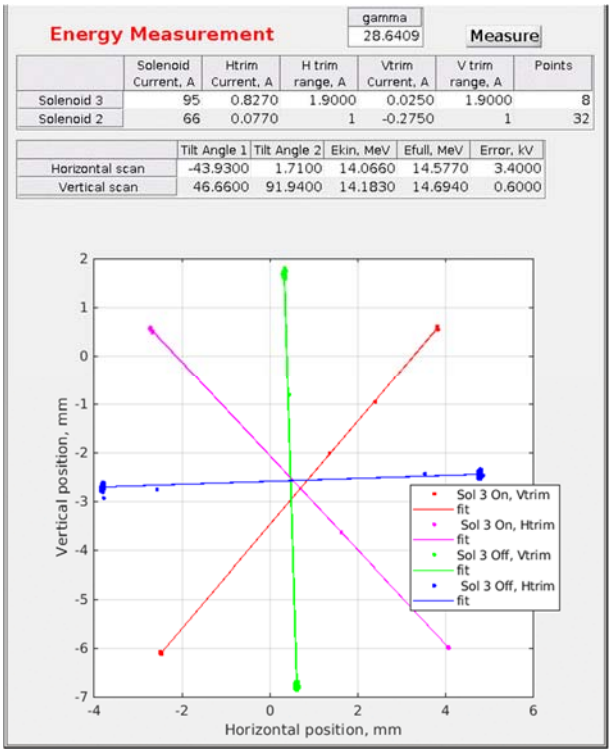

Figure 7: An example of the energy measurement of the electron beam in the cooling section.

Beam based alignment in the cooling section

Accurate alignment of the electron beam with the ion beam in the cooling section is crucial for demonstrating CeC. As shown in fig. 8, the longitudinal alignment of the two beam is achieved by overlapping the signals induced by the two beams in a common bpm in the cooling section.

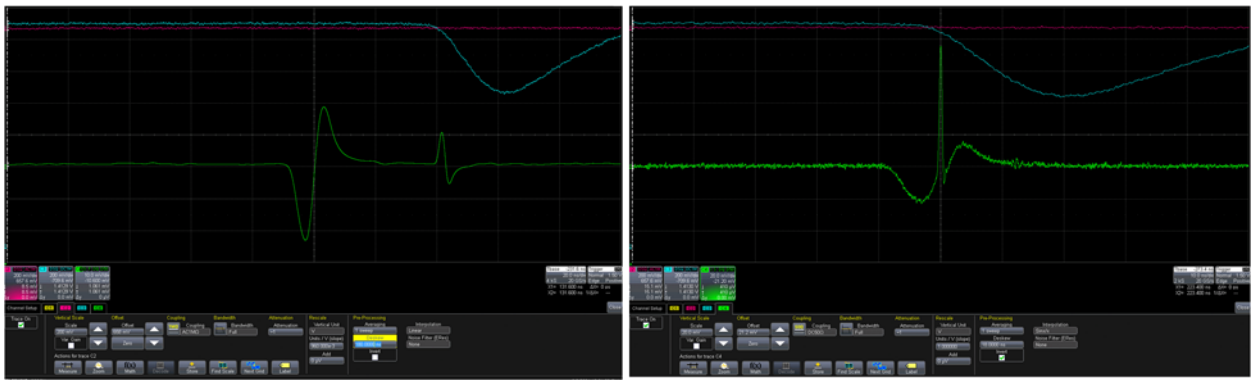

Figure 8: Longitudinal alignment of the electron bunch with the ion bunch. The green traces in the screenshots are the signals picked up from a bpm in a common section. (Left) the ion bunch and electron bunch are separate. The pulse on the left with is induced by the ion bunch and that on the right is induced by the electron bunch. (Right) the electron bunch and the ion bunch are overlapping.

To align the electron beam with the ion beam transversely, we first need to define the orbit for the ion beam through the cooling section. There are two quadrupoles dedicated for this purpose. One of the quadrupoles is located near the entrance of the cooling section and the other is close to the exit of the cooling section. By monitoring and minimizing the orbit change in all RHIC bpms induced by the current changes in these quadrupoles, we were able to put the ion beam through the centers of the two alignment quadrupoles. Fig. 9 shows the orbit variation of the ion beam induced by varying the quadrupole current before (Left) and after (Right) threading the ion beam through the center of the alignment quadrupoles.

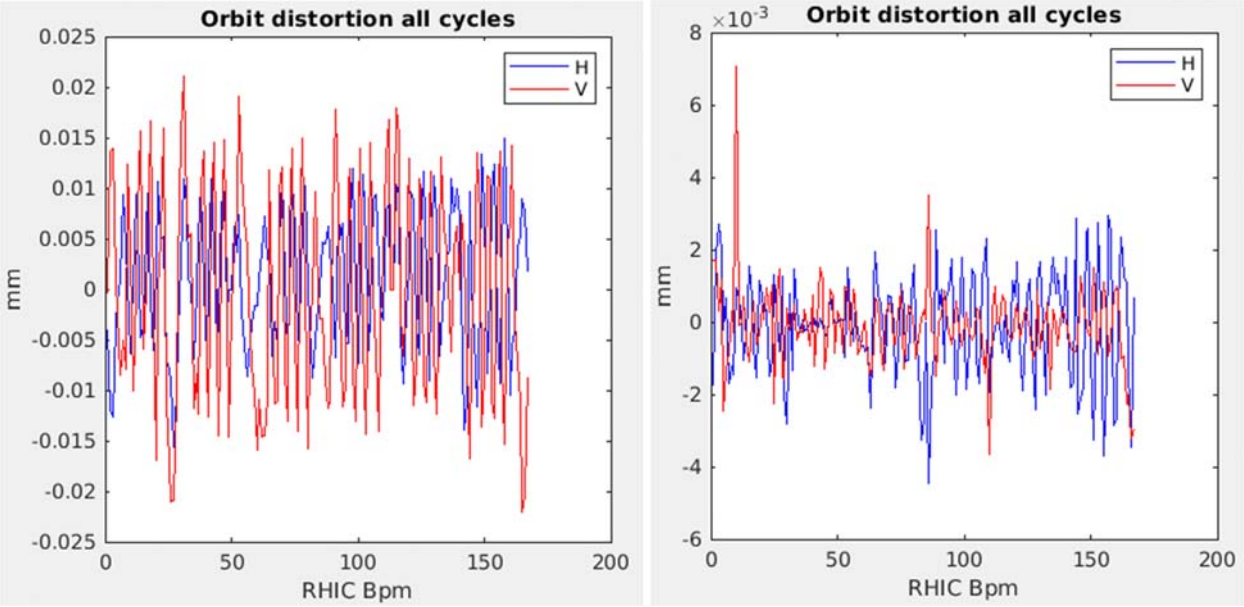

Figure 9: Threading the ion beam through the centers of the alignment quadrupoles in the CeC cooling section. (Left) the orbit changes in all RHIC BPMs induced by changing the downstream alignment quadrupole from -0.3 A to 0.3 A at 4 GeV RHIC operation.

After the orbit of the ion beam is defined in the cooling section, we measured the offsets and tilts of all seven CeC solenoids by monitoring how the ion beam orbit around RHIC changes with the current in each CeC solenoid and minimizing the orbit changes with two CeC trims in each plane. Fig. 10 shows an example of correcting the orbit change of the ion beam around the RHIC ring due to the CeC solenoid with two CeC trims in each transverse plane. The offsets and tilts of the solenoids can then be calculated through the strength of the required trim strength for the correction. Based on the measured data, we went into the RHIC tunnel and adjusted the positions and orientations of all seven solenoids so that their axis are along the trajectory of the ion beam as defined by the alignment quadrupoles.

The final step is to thread the electron bunch through the centers of all seven CeC solenoids in the cooling section, which is achieved by similar procedures applied in the LEBT section of the CeC system, i.e. calculating the offset and orbital angle of the electron beam at the location of the solenoid from its orbit change at the downstream bpm or YAG screen induced by scanning

the solenoid current and then applying orbit corrections accordingly. Fig. 11 shows one example of threading the electron beam through the center of a CeC solenoid in the cooling section.

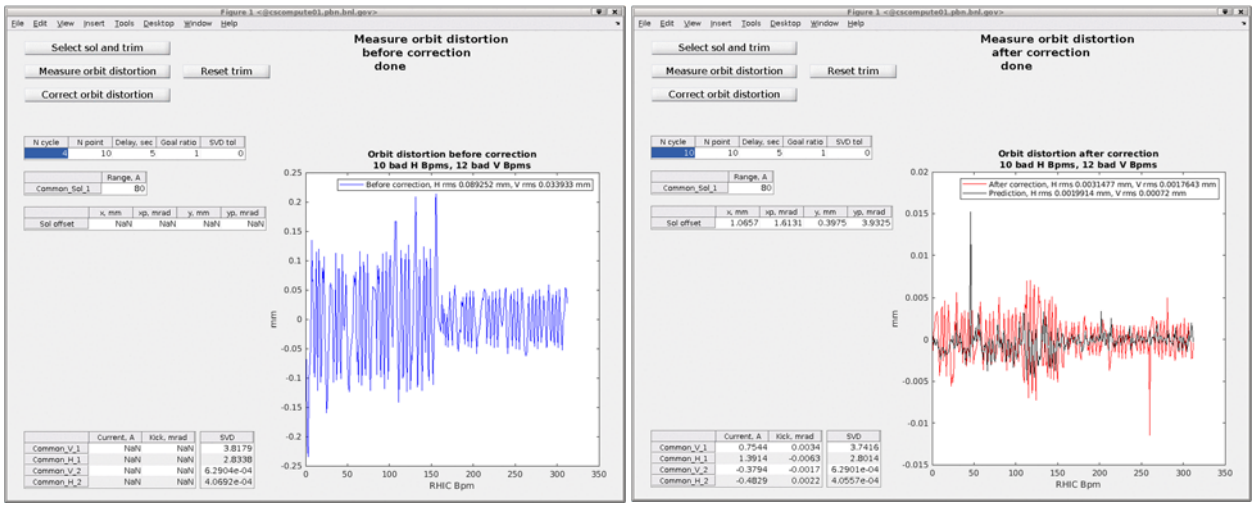

Figure 10: An example of measuring the offset and tilt of the CeC solenoid with respect to the trajectory of the ion beam. (Left) The change of the ion beam orbit around the RHIC ring due to change of the CeC solenoid without correction from the CeC trims; (Right) Similar to the left plot but with correction from the CeC trims.

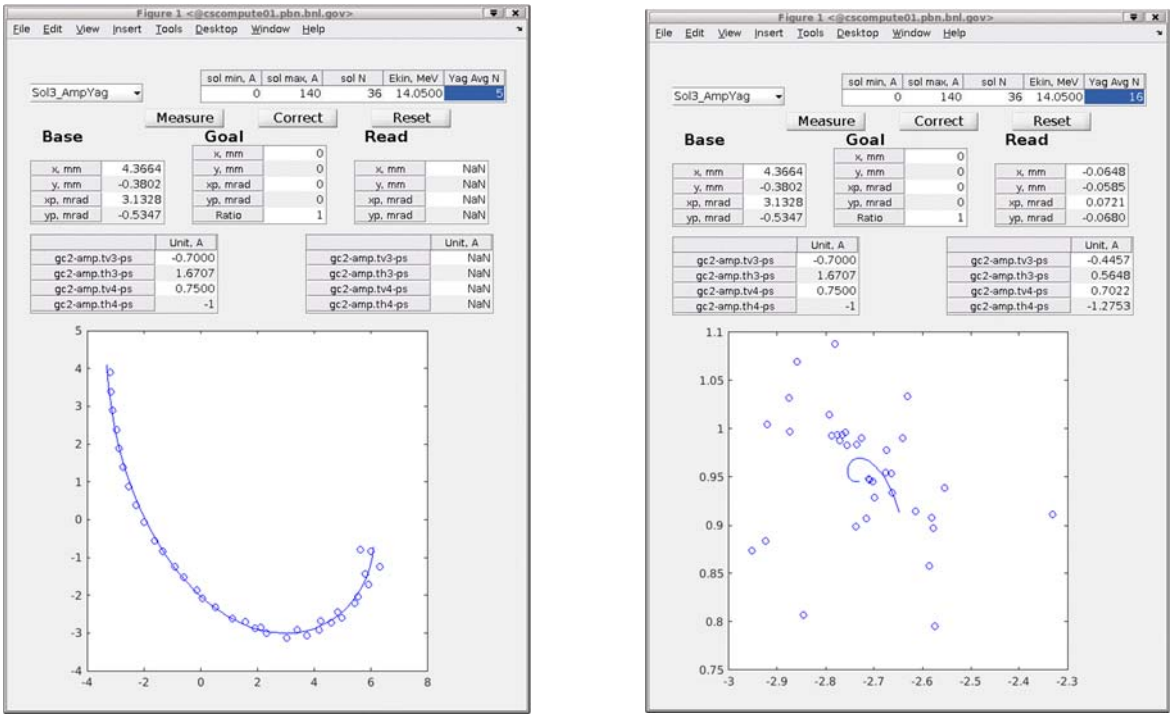

Figure 11: An example of threading the electron beam through the center of the CeC solenoid in the cooling section. (Left) beam position variation at the common section YAG screen due to changes in the solenoid current before orbit correction; (Right) beam position variation at the common section YAG screen due to changes in the solenoid current after orbit correction.

As we will see in the later sections, the observations of the recombination signal and the slow longitudinal cooling of the ion beam confirmed that the procedure for the alignment of the two beams worked successfully.

Recombination signal and the observation of the longitudinal cooling

During the CeC experiment in run 21, we were able to observe a clear signal from the recombination monitor for the first time which indicated that the alignment of the two beams were reasonable in all 6 dimensions. As shown in fig. 12, the recombination signal of the ion bunch overlapping with the electron bunch were higher than the witness bunches by a factor of 3 to 8.

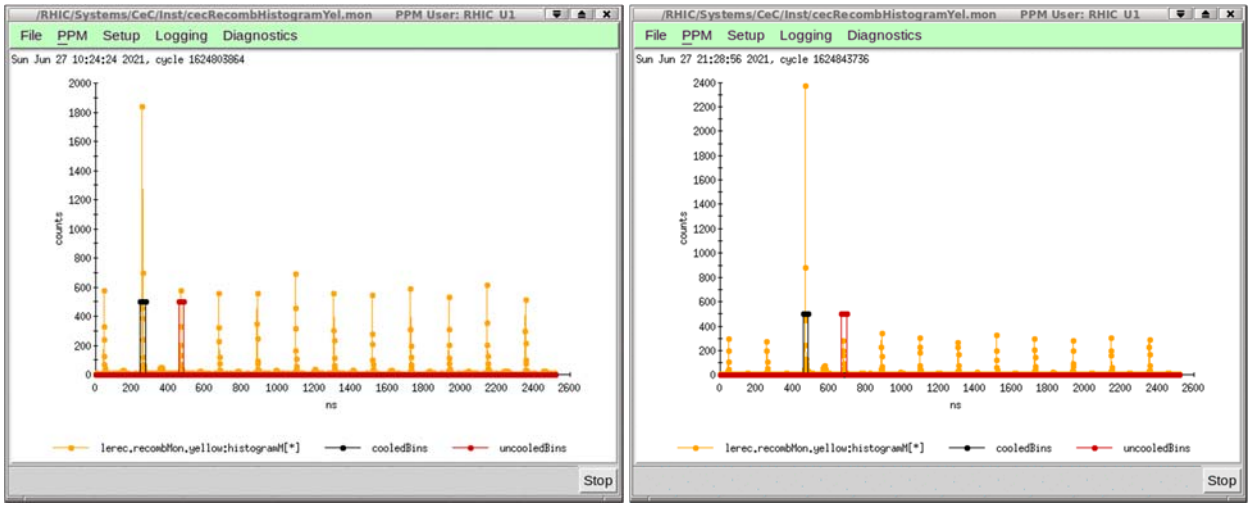

Figure 12: Recombination observed during the CeC experiment in run 21. (Left) the electron bunch is aligned with the second ion bunch in the bunch train consisting of 12 ion bunches. The other 11 bunches are witness bunches which do not interacting with the electrons. (Right) the electron bunch is aligned with the third ion bunch in the bunch train.

Fig. 13 (Right) shows how the peak of the recombination rate varies with the energy of the electron beam, which qualitatively agrees with the theoretical calculation (Left) if we assume that there is an alignment error of the transverse orbital angle of the electron beam in the order of 0.8 mrad [1].

Since June. 27, we had observed slow longitudinal cooling of the ion bunch and fig. 14 shows one example of such observation in July 2. The observed cooling time was in the range of 100 hours and was not as sensitive as what expected for the CeC. In addition, the cooling remained after we turned off the CeC amplification by relaxing the solenoids in the PCA section. The cooling time is consistent with what expected for the traditional electron cooling with an angular spread or orbital angle in the range of 1 mrad. These observations from the observed cooling suggests

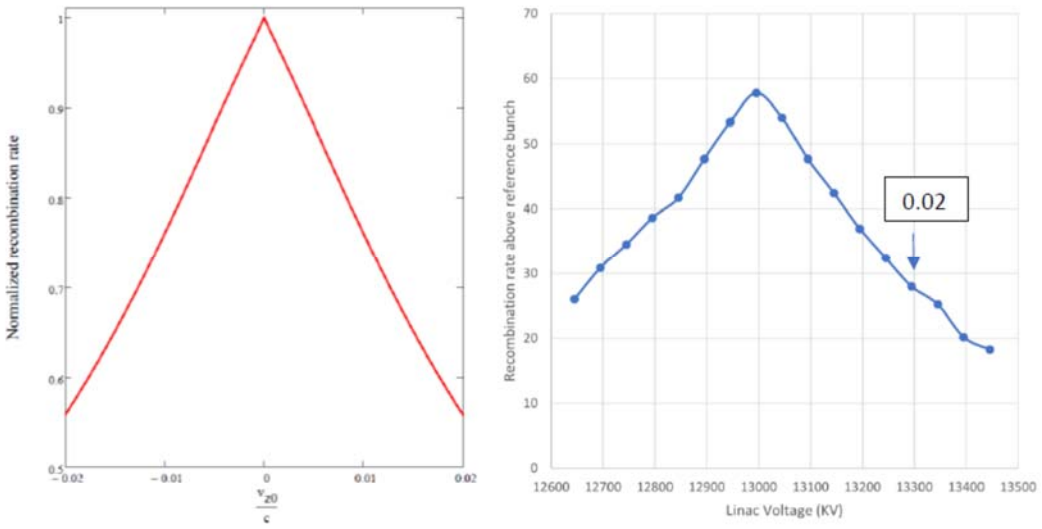

Figure 13: comparison of recombination rate as predicted from analytical calculation and that measured in CeC experiment. (Left) normalized recombination rate as a function of v_{z0}/c for transverse angular spread of 0.3 mrad and horizontal orbit angle of 0.8mrad; (Right) measured recombination rate in CeC experiment.

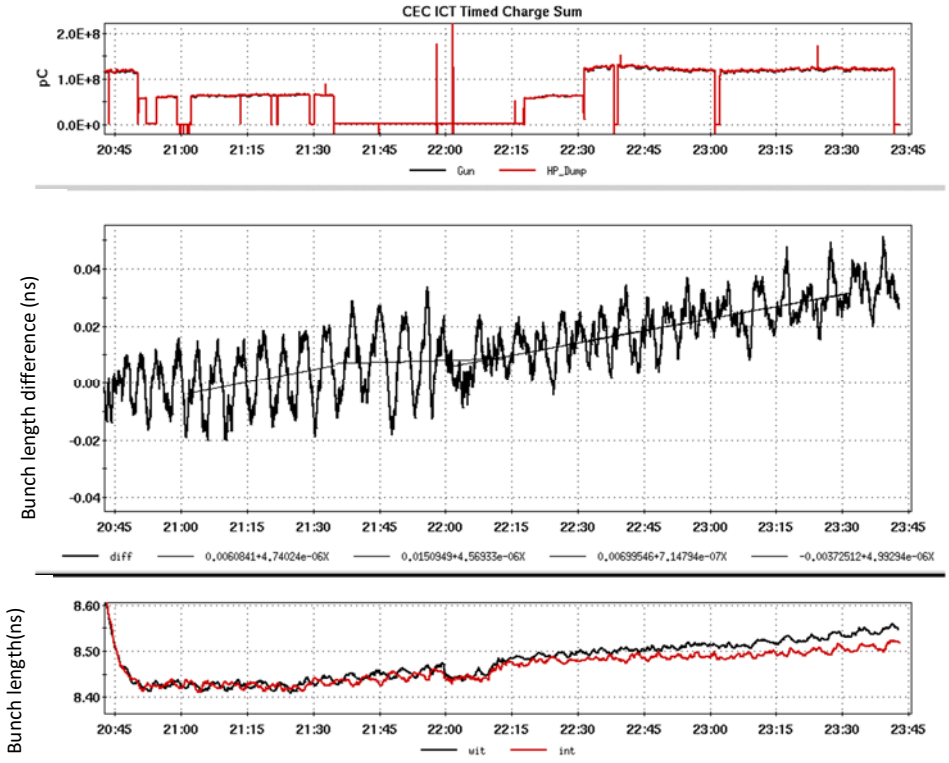

Figure 14: Observation of slow longitudinal cooling in the CeC experiment during run 21 (7/2/21). (Top) total charge of the electron bunch train; (Bottom) the FWHM bunch length of the witness ion bunch (black) and the ion bunch interacting with the electron beam. (Middle) the bunch length of the witness ion bunch subtracted by that of the interacting ion bunch.

that the observed cooling is the traditional electron cooling.

Challenges for demonstrating the CeC

The main challenge of the CeC experiment identified in run 21 was the bunch-by-bunch energy jitter in the electron beam with a peak-to-peak amplitude of 0.35%, as shown in fig. 15. Our understanding is that the energy jitter was caused by the timing jitter in the laser pulses which had the peak-to-peak amplitude of 100 ps. There was also jitter in the laser power with a level of 10%. According to our estimates, the energy jitter alone will reduce the cooling rate by a factor of 125 and hence it is critical to find a solution for reducing the timing jitter and the intensity jitter of the laser by a factor of 4.

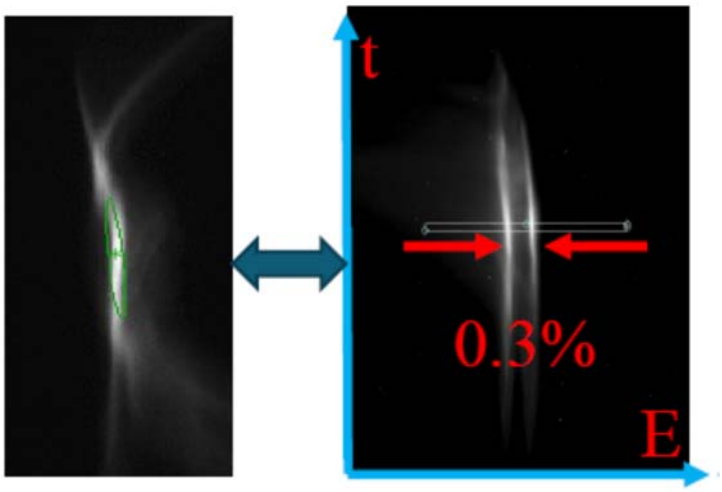

Figure 15: The longitudinal phase space image as observed in the diagnostic YAG 2 of the TRDBL for an electron train consisting of two electron bunches. The longitudinal phase space image was constantly jumping and the pictures shows two examples of the images.

In addition to the bunch-by-bunch energy jitter, we also observed slow energy drift in the level of 0.1 % which was likely caused by the residue dependance of the RF voltages and phases on the ambient temperature. We need to develop reliable feedbacks to compensate for these energy drifts. In order to evaluate the PCA gain, we also need a cryo-cooled IR detector and very large RFI in the IP2 diagnostics cables which need be addressed before the start of run 22.

There are a number of improvements required for successful demonstration of the CeC in Run 22, including orbit feedback, reliable slice emittance measurements, solving noise problem in the CeC diagnostics as well as modification of the CeC systems (removing unnecessary cavity, new trims and undulator, new profile monitor and pepper-pot).

We lost at least 7 weeks of operation from severely damage to the SRF electron gun. Although we were lucky to restore the gun operation every time when the gun failed, it took significant

time and effort for its recovery from contamination. Particulate-free preparation of photo-cathodes with uniform QE is one of the challenge that we need to solve before run 22.

Summary

Significant progresses has been made during the CeC experiment in run 21 including commissioning the new TRDBL, developing new techniques for measuring electron beam energy at the common section, developing the procedure for the alignment of the electron beam with the ion beam, observing the recombination signal generated in the CeC cooling section and observing the traditional electron cooling with the CeC system. However, there were significant challenges for observing the CeC, including the bunch-by-bunch energy jitter, lacking of a sensitive IR detector, slow energy drifting of the electrons, the jitters in the laser (timing and power) and the frequent gun failure due to multipacting. In order to achieve our goal of demonstrating the CeC in run 22, these issues must be resolved before the start of the run.

REFERENCES

[1] G. Wang, '*Influences of the transverse motions of the particles to the recombination rate of a co-propagating electron-ion system*', Report No. C-A/AP/651 (2021).